High-Latitude Dinosaur Nesting Strategies during the Latest Cretaceous in North-Eastern Russia

Romain Amiot, Lina B Golovneva, Pascal Godefroit, Jean Goedert, Géraldine Garcia, Christophe Lécuyer, François Fourel, Alexei B Herman, Robert A Spicer

diversity

MDPI

Article

High-Latitude Dinosaur Nesting Strategies during the Latest Cretaceous in North-Eastern Russia

Romain Amiot [1,*], Lina B. Golovneva [2], Pascal Godefroit [3], Jean Goedert [4], Géraldine Garcia [5], Christophe Lécuyer [1], François Fourel [6], Alexei B. Herman [7] and Robert A. Spicer [8,9]

1 Laboratoire de Géologie de Lyon, Terre, Planètes et Environnement (LGL-TPE), Université Claude Bernard Lyon1/CNRS UMR 5276/École Normale Supérieure de Lyon, 69622 Villeurbanne, France
2 V.L. Komarov Botanical Institute, Russian Academy of Sciences, 197376 St. Petersburg, Russia
3 Directorate 'Earth and History of Life', Royal Belgian Institute of Natural Sciences, rue Vautier 29, B-1000 Brussels, Belgium
4 Muséum National d'Histoire Naturelle, Centre de Recherche en Paléontologie–Paris (CR2P), CNRS/MNHN/Sorbonne Université, CP 38, 57 rue Cuvier, 75231 Paris, France
5 IPHEP, UMR CNRS 7262, Université de Poitiers, UFR SFA, Bat. B35, 6 rue M. Brunet, TSA 51106, CEDEX 9, 86073 Poitiers, France
6 Laboratoire d'Ecologie des Hydrosystèmes Naturels et Anthropisés LEHNA UMR CNRS 5023, Université Claude Bernard Lyon 1, 69100 Villeurbanne, France
7 Geological Institute, Russian Academy of Sciences, 119017 Moscow, Russia
8 CAS Key Laboratory of Tropical Forest Ecology, Xishuangbanna Tropical Botanical Garden, Chinese Academy of Sciences, Mengla 666303, China
9 School of Environment, Earth and Ecosystem Sciences, The Open University, Milton Keynes MK7 6AA, UK
* Correspondence: romain.amiot@univ-lyon1.fr

Abstract: Dinosaur eggshell fragments attributed to the oofamilies Spheroolithidae and Prismatoolithidae and recovered from the latest Cretaceous Kakanaut Formation of North-eastern Russia (Chukotka) constitute one of the northernmost records of dinosaur reproductive behaviors. The high palaeolatitude of the locality (~75° N), as well as the cool near-polar climate, where summer temperatures only averaged 20 °C during the warmest month, dark near-freezing winters and egg incubation that could have lasted several months, raise questions about dinosaur reproductive strategies, particularly in terms of the timing of egg laying. In order to investigate seasonal aspects of Kakanaut dinosaur reproductions, carbonate from eggshell fragments have been analyzed for their oxygen and carbon isotope compositions, along with the oxygen and carbon isotope compositions of apatite phosphate and structural carbonate of associated theropod, hadrosaur and ankylosaur teeth as well as lepisosteid fish scales. Stable oxygen and carbon isotope compositions of eggshells from the Kakanaut Formation together with those of associated adult dinosaur teeth and fish scales reveal differences in mineralization timing between eggshells and teeth and show that eggs were laid at the very beginning of spring when snowmelt drained from nearby highlands. We propose that Kakanaut dinosaurs laid their eggs at the very beginning of spring in order to accommodate an incubation period that lasted several months. This timing would also benefit from mild temperatures and increasing food availability when the eggs hatch, allowing the hatchlings to grow large enough to survive the next winter or perhaps follow adult animals in their migration southwards.

Keywords: dinosaur; reproduction; near-polar latitudes; oxygen isotopes; carbon isotopes

Citation: Amiot, R.; Golovneva, L.B.; Godefroit, P.; Goedert, J.; Garcia, G.; Lécuyer, C.; Fourel, F.; Herman, A.B.; Spicer, R.A. High-Latitude Dinosaur Nesting Strategies during the Latest Cretaceous in North-Eastern Russia. *Diversity* **2023**, *15*, 565. https://doi.org/10.3390/d15040565

Academic Editor: Federico Agnolin

Received: 7 March 2023
Revised: 11 April 2023
Accepted: 12 April 2023
Published: 17 April 2023

1. Introduction

Climate and especially seasonality act as major constraints on the reproductive strategies of reptiles (*sensus* Sauropsida) in terms of egg-laying periods [1] and egg incubation method [2]. In turn, reproductive ecologies limit the geographic distribution of reptiles in terms of latitudinal range and environments [2,3]. Some of the most challenging environments for successful reproduction are in near-polar regions, where extended periods

of darkness and freezing winters reduce habitability and limit food availability to a few months between spring and autumn. Extant birds living at high latitudes as permanent residents, such as the North American white-winged crossbill (*Loxia leucoptera*), the great horned owl (*Bubo virginianus*) or the bald eagle (*Haliaeetus leucocephalus*), adapt their breeding strategy by either laying eggs during the harshest part of the winter so they hatch at the very beginning of the plant growing season or by adopting opportunistic breeding periods depending on the shift of seasons [4–6]. Due to their exceptional range of body mass, from a few grams to several tens of tons, non-avian dinosaurs might have had various reproductive strategies adapted to their physiological and anatomical peculiarities [7]. Paleoclimate studies document that such harsh near-polar conditions existed during the Cretaceous [8–10].

Based on these considerations, the discovery of dinosaur remains from Cretaceous high palaeolatitude sites in Alaska, North-eastern Russia and Australia raises questions as to whether they were able to live in near-polar regions year-round and how they reproduced or had to migrate seasonally [11–13]. Recent discoveries of eggshell fragments in North-eastern Russia [11], as well as perinatal and very young individuals from Alaska [14,15], demonstrates that some dinosaurs, including large-sized species, were able to successfully reproduce at high latitudes and were most likely permanent residents of high latitudes. As large dinosaurs such as hadrosaurs and tyrannosaurids were likely not able to brood their eggs like smaller theropods such as oviraptorosaurids [16,17], they had to rely on external sources of heat, such as solar irradiance or heat produced by the decay of plant debris, to warm their nests to an appropriate temperature for incubation. In the context of ecological and climatic constraints, along with egg incubation that could have lasted from a few weeks up to six months depending on the species [18,19], it seems likely that high-latitude dinosaurs had to optimize the timing of their egg laying in order for their hatchlings to have enough food to grow up sufficient to survive the next winter.

Seasonal aspects of egg laying can be investigated using the oxygen isotope composition of eggshell carbonate ($\delta^{18}O_c$) compared to that of adult teeth phosphate ($\delta^{18}O_p$). Indeed, the $\delta^{18}O$ value of vertebrate mineralized tissues (bones, teeth, scales or eggshell) reflects the oxygen isotope composition of the animal body water with an isotopic fractionation that depends on body temperature [20,21]. In turn, the $\delta^{18}O$ value of the body water of vertebrates is controlled by that of the oxygen inputs (drinking and food water, oxygen in food and breathed oxygen) and outputs (water vapor exhaled and lost through transcutaneous evaporation and water in urine and feces), with some of these oxygen fluxes being associated with isotope fractionation [22,23]. By applying appropriate oxygen isotope fractionation established between mineralized tissue (phosphate or carbonate) and ingested water, it is possible to estimate the oxygen isotope composition of local surface waters ($\delta^{18}O_w$) within the vertebrate living environment [24,25]. Continental surface waters, such as ponds and streams, are derived principally from local meteoric waters, but larger rivers and lakes can mix waters from distant origins within the water catchment, including high-altitude ^{18}O-depleted snowmelt from nearby mountains. Because the $\delta^{18}O$ value of meteoric waters is controlled by air temperature and the amount of precipitation [26], the oxygen isotope composition of surface waters varies seasonally, and these variations can be recorded in the hard tissues of vertebrates that mineralize incrementally [27]. Moreover, precipitation of eggshell calcite takes place over only a few hours to a few tens of hours for each egg. Thus, the oxygen isotope composition of eggshell calcite records a very short period of water ingestion by the female, corresponding to the residency time and turnover rate of body water. This residency time varies from a few days to a few weeks depending on the body mass of the female.

The carbon isotope composition of eggshell calcite or the apatite-bound carbonate of bones or teeth ($\delta^{13}C_c$) belonging to air-breathing vertebrates reflects that of their diet, with a carbonate-diet ^{13}C enrichment that depends on their digestive physiology [28]. Plant-eating animals have a $\delta^{13}C_c$ value that depends on the carbon isotope composition of consumed plant tissues, the latter having $\delta^{13}C$ values mainly controlled by that of atmospheric

CO_2 and with a carbon isotope fractionation that depends on the plant photosynthetic pathway [29]. The C_3 pathway is the most common one, occurring in all trees, most shrubs, herbs and grasses in regions with a cool growing season. C_4 photosynthesis operates in grasses from regions with a warm growing season and in some sedges and dicots. Finally, crassulacean acid metabolism (CAM) occurs in succulent plants. C_4 and CAM plants were most likely absent in Late Cretaceous ecosystems [30] and they will not be discussed any further. Today, C_3 plants have a mean $\delta^{13}C$ value of −27‰ V-PDB (ranging from −35‰ to −22‰), reflecting both the $\delta^{13}C$ value of atmospheric carbon dioxide and local environmental conditions [31]. Indeed, abiotic factors, such as water and osmotic stress, variations in light intensity, local temperature and pCO_2, influence the carbon isotope compositions of C_3 plants by affecting leaf stomatal conductance, which, in turn, constrains the magnitude of CO_2 diffusion through the plant epidermis. All these factors result in variations in the $\delta^{13}C$ values found in C_3 plants [29].

Knowing the apatite-diet carbon-heavy isotope enrichment ($\Delta^{13}C_{ap\text{-}diet}$) of plant-eating vertebrates, it is thus possible to estimate the carbon isotope compositions of their ingested local plants from the $\delta^{13}C_c$ value of their bone or tooth apatite carbonate [28], as well as of their eggshell calcite [32]. For extinct dinosaurs, apatite-diet ^{13}C enrichments of about +18‰ have been estimated for two ornithischians, ceratopsians and hadrosaurs [33,34], and about +15–16‰ for the sauropods [35,36].

Based on the above considerations, we interpret the stable oxygen and carbon isotope compositions of dinosaur eggshell calcites and tooth apatites in terms of environmental conditions and timing of egg laying. We then discuss the possible reproductive strategies used by near-polar dinosaurs in the northeast of Russia during the latest Cretaceous.

2. Material and Method

Dinosaur teeth, eggshell fragments and fish scales were sampled for stable isotope analysis (Figure 1). They were collected from the Koryak Upland region of North-eastern Russia, in a volcaniclastic sedimentary succession comprising the Kakanaut Formation exposed along the Kakanaut River. This formation is a 1000 m thick continental sequence, the exact age of which is still debated. The bone-bearing layers are either dated as (1) early late Maastrichtian considering that the formation is underlain by marine deposits of late Maastrichtian age and overlain by marine sediments of the Kokuy Unit, which contain poorly preserved plant fossils and the latest Maastrichtian invertebrate fauna [10,37,38] or (2) late Campanian–early Maastrichtian considering that underlying and overlapping deposits do not directly contact marine layers containing stratigraphically important forms of mollusk fossils. Furthermore, the dinosaur remains were found together with plant representative of the Kakanaut flora, allowing the assignment of the bone- and plant-bearing layers to the Gornaya River phytostratigraphic horizon dated as late Campanian, possibly early Maastrichtian [39]. During the latest Cretaceous, the Koryak Upland region was situated at a paleolatitude of about 75° N [40] (Figure 1).

The studied material consists of two hadrosaurid, three ankylosaurid and two theropod teeth, three spheroolithid and two prismatoolithid eggshell fragments and three lepisosteid fish scales, all collected from a single highly fossiliferous lens [11]. When possible, enamel was extracted from the teeth and ground into fine powder using a microdrill but, for smaller teeth, scales and eggshell fragments, whole specimens were ground using an agate mortar and pestle (Table 1).

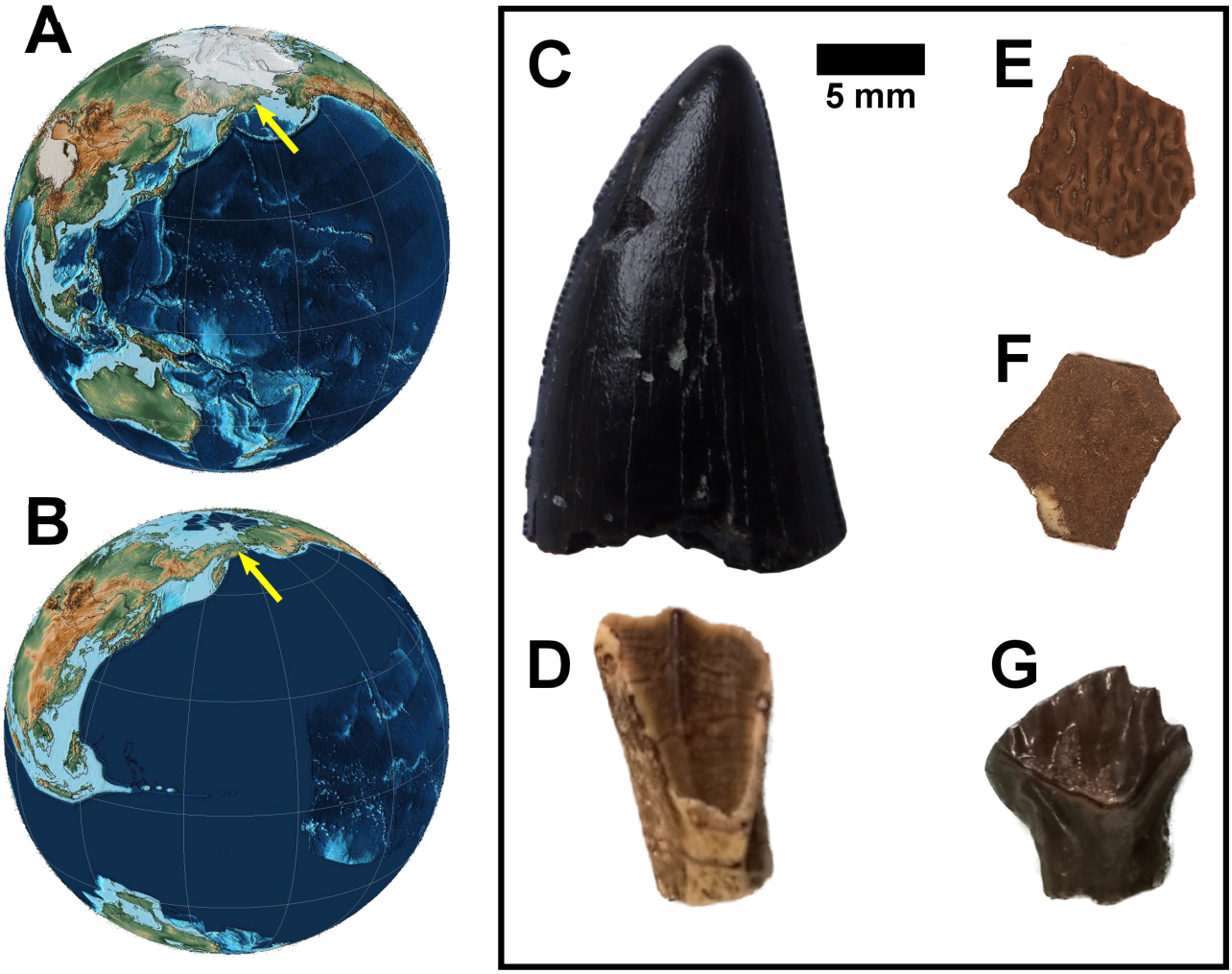

Figure 1. Present-day (**A**) and latest Cretaceous (**B**) position of the Kakanaut area plotted as a yellow arrow on a paleogeographic reconstruction [41]. (**C**–**G**): example of analyzed teeth and eggshells, including the tyrannosaurid tooth KK12 (**C**), the hadrosaurid tooth KK06 (**D**), a spheroolithid (**E**) and prismatoolithid (**F**) eggshell fragments, and an ankylosaurid tooth KK08 (**G**).

Table 1. Carbon and oxygen isotope compositions of apatite phosphate ($\delta^{18}O_p$) and carbonate ($\delta^{13}C_c$, $\delta^{18}O_c$) and eggshell calcite from vertebrates reported along with the weight percent of apatite-bound carbonate, sample number, apatite material and taxonomy. The last column corresponds to the oxygen isotope composition of water ($\delta^{18}O_w$) estimated from the $\delta^{18}O_p$ value of tooth apatite phosphate or the $\delta^{18}O_c$ value of eggshell calcite using existing fractionation equations (see text).

Sample	Material	Taxon	$\delta^{18}O_p$ ‰ V-SMOW	$\delta^{18}O_c$ ‰ V-SMOW	$\delta^{13}C_c$ ‰ V-PDB	CO_3 Content WT%	$\delta^{18}O_w$ ‰ V-SMOW
KK05	tooth enamel	Hadrosaurid indet.	12.9	21.0	−2.4	6.9	−9.8
KK06	tooth enamel	Hadrosaurid indet.	22.6	28.5	−5.2	5.9	1.0
KK07	tooth bulk	Ankylosauria indet.	14.9	22.0	−0.8	8.6	−7.5
KK08	tooth bulk	Ankylosauria indet.	14.7	21.3	0.8	8.2	−7.8
KK09	tooth bulk	Ankylosauria indet.	14.8	21.9	1.0	6.2	−7.6
KK10	3 bulk scales	lepisosteidae indet.	14.2				
KK11	tooth enamel	Theropoda indet.	9.6	18.8	−7.8	4.4	−13.5
KK12	tooth enamel	Tyrannosauridae indet.	10.6	18.7	−7.1	5.0	−12.3
KK19	eggshell calcite	Spheroolithidae		16.4	−12.7		−17.0
KK20	eggshell calcite	Spheroolithidae		20.2	−12.9		−12.9
KK21	eggshell calcite	Spheroolithidae		20.8	−12.1		−12.2

Table 1. *Cont.*

Sample	Material	Taxon	$\delta^{18}O_p$ ‰ V-SMOW	$\delta^{18}O_c$ ‰ V-SMOW	$\delta^{13}C_c$ ‰ V-PDB	CO_3 Content WT%	$\delta^{18}O_w$ ‰ V-SMOW
KK22	eggshell calcite	Prismatoolithidae		18.4	−8.5		−14.8
KK23	eggshell calcite	Prismatoolithidae		20.2	−9.2		−12.8
Serial sampling of tooth KK12 (Goedert et al. [22])							
Sample	**Material**	**Taxon**	$\delta^{18}O_p$ ‰ V-SMOW	**Dist. from Apex (mm)**			$\delta^{18}O_w$ ‰ V-SMOW
R0	tooth enamel	Tyrannosauridae indet.	10.7	21			−12.2
R1	tooth enamel	Tyrannosauridae indet.	11.0	19			−11.9
R1a	tooth enamel	Tyrannosauridae indet.	10.7	17			−12.3
R2	tooth enamel	Tyrannosauridae indet.	10.3	15			−12.7
R2a	tooth enamel	Tyrannosauridae indet.	10.3	13			−12.7
R3	tooth enamel	Tyrannosauridae indet.	10.7	11			−12.3
R3a	tooth enamel	Tyrannosauridae indet.	11.1	9			−11.8
R4	tooth enamel	Tyrannosauridae indet.	11.9	7			−10.9
R4a	tooth enamel	Tyrannosauridae indet.	10.7	5			−12.2
R5	tooth enamel	Tyrannosauridae indet.	10.4	2			−12.6

Apatite samples were prepared following the wet chemistry protocol described in Lécuyer [42]. For each sample, an aliquot of 30 mg of apatite powder was dissolved in 2 mL of 2 M HF. The CaF_2 residue was separated by centrifugation and the solution neutralized by adding 2.2 mL of 2 M KOH. Amberlite™ anion-exchange resin beads were added to the solution to isolate the PO_4^{3-} ions. After 24 h, the solution was removed, the resin was rinsed and eluted with 27.5 mL of 0.5 M NH_4NO_3 for 4 h. Then, 0.5 mL of NH_4OH and 15 mL of an ammonia solution of $AgNO_3$ were added and the solutions were placed in a thermostatic bath at 70 °C for 7 h, allowing the slow and quantitative precipitation of Ag_3PO_4 crystals. Oxygen isotope compositions of silver phosphate crystals were measured using a varioPYROcube Elemental Analyzer interfaced in continuous flow mode to an Isoprime Isotopic Ratio Mass Spectrometer. For each sample, 5 aliquots of 300 µg of Ag_3PO_4 were mixed with 300 µg of pure graphite powder loaded in silver foil capsules. Pyrolysis was performed at 1450 °C. Measurements have been calibrated against silver phosphate precipitated from the NBS120c (natural Miocene phosphorite from Florida), as well as with the NBS127 (barium sulfate precipitated using seawater from Monterey Bay, CA, USA). The value of NBS120c was fixed at 21.7‰ (V-SMOW; Vienna Standard Mean Ocean Water) according to Lécuyer et al. [43] and that of NBS127 set at the value of 9.3‰ V-SMOW [44] for correction of instrumental mass fractionation during CO isotopic analysis. Silver phosphate precipitated from standard NBS120c along with the silver phosphate samples derived from fossil bioapatites were repeatedly analyzed ($\delta^{18}O_p$ = 21.70 ± 0.30‰, n = 4) to ensure that no isotopic fractionation occurred during the wet chemistry. Data are reported as $\delta^{18}O$ values vs. V-SMOW (in ‰ δ units).

In order to remove potential organic contaminant as well as secondarily precipitated calcite, aliquots of about 10 mg of apatite powder were treated using the protocol of Koch et al. [45]. Powders were reacted with a 2% NaOCl solution to remove organic matter, then rinsed five times with double deionized water and air-dried at 40 °C for 24 h. Acetic acid (0.1 M) was then added and left for 24 h, after which the powder was again rinsed five times with double deionized water and air-dried at 40 °C for 24 h. For both treatments, the powder/solution ratio was kept constant at 0.04 g mL^{-1}. The measurements were performed using an isoFLOW system connected online in continuous flow mode to a precisION mass spectrometer. For each sample, two aliquots of 2 mg of pretreated apatite and 300 µg of eggshell calcite powders were loaded in 3.7 mL soda glass vials, round bottomed with exetainers caps, and were reacted with oversaturated anhydrous phosphoric acid. The reaction took place at 90 °C in a temperature regulated sample tray. The CO_2 gas generated during the acid digestion of the carbonate sample was then transferred to the mass spectrometer via a centrION interface. Calibrated CO_2 gas was used as a monitoring gas. Typical reproducibility was 0.05‰ and 0.07‰ for

$\delta^{13}C$ and $\delta^{18}O$ measurements, respectively. The calibrated materials used were Carrara Marble ($\delta^{18}O_{V\text{-}PDB}$ = −1.84‰; $\delta^{13}C_{V\text{-}PDB}$ = +2.03‰; [46]) and NBS18 ($\delta^{18}O_{V\text{-}PDB}$ = −23.2‰; $\delta^{13}C_{V\text{-}PDB}$ = −5.01‰). Isotopic compositions are quoted in the standard δ notation relative to V-PDB for carbon and V-SMOW for oxygen.

3. Results

Dinosaur teeth and eggshell, as well as fish scale oxygen and carbon isotope compositions are given in Table 1. The oxygen isotope composition of environmental water calculated using apatite phosphate-water [24] as well as eggshell calcite-water [25] oxygen isotope fractionation equations for birds (dinosaur extant relatives) are also provided in Table 1. Interestingly, environmental waters estimated from eggshell calcite have the lowest $\delta^{18}O_w$ values from −17.0‰ to −12.2‰, theropod dinosaurs have intermediate $\delta^{18}O_w$ values of −13.5‰ and −12.3‰, and plant-eating hadrosaurids and ankylosaurs have higher $\delta^{18}O_w$ values ranging from −9.8‰ to −7.5‰. It is worth noting that the hadrosaurid tooth KK06 yielded a $\delta^{18}O_w$ value of +1.0‰, corresponding to a highly evaporated water source.

Carbon isotope compositions of dinosaur teeth and eggshells seem to be grouped by mineralized tissue type and taxonomy. Eggshells have the lowest $\delta^{13}C_c$ values, ranging from −12.9‰ to −12.1‰ for hadrosaurids (Spheroolithidae) and from −9.1‰ to −8.5‰ for theropods (Prismatoolithidae), while tooth apatite carbonate values are also ordered with theropods having $\delta^{13}C_c$ values ranging from −7.8‰ to −7.1‰, hadrosaurids ranging from −5.2‰ to −2.4‰ and ankylosaurids from −0.8‰ to +1.0‰.

4. Discussion

4.1. Primary Preservation of the Carbon and Oxygen Isotope Compositions of Tooth Apatite and Eggshell Calcite

Based on the following considerations, it is assumed that both carbon and oxygen of tooth apatite and eggshell calcite have preserved at least part of their pristine stable isotope compositions:

1. Oxygen isotope compositions of tooth phosphate show a large range of variation from 9.6‰ to 22.6‰, precluding any re-equilibration with diagenetic fluids that would tend to homogenize the oxygen isotope compositions of phosphate towards a possible diagenetic end member [47].
2. Oxygen isotope compositions of tooth phosphate and corresponding structural carbonate are linearly correlated with a slope close to unity and an offset of 6‰ to 9‰ (Figure 2). This matches the expected fractionation of 8–9‰ observed between phosphate and carbonate in extant vertebrates [48–50].
3. The relative amount of carbonate in dinosaur apatites estimated from the measured CO_2 peak intensity of the mass spectrometer ranges from 4.4 Wt% (weight percent) to 8.6 Wt% (Table 1), within the expected range of 2–13 Wt% measured in extant vertebrates [51–53]. A higher amount would have indicated a contamination of the apatite carbonate stable isotope compositions with diagenetic calcite that would not have been removed during the chemical cleaning.
4. No correlation is observed between the carbon and oxygen isotope compositions of eggshell calcite that would hint to a partial re-equilibration with environmental diagenetic fluids [54].
5. Instead, a significant isotopic clustering is observed among analyzed taxa (Figure 3) and supports the preservation of an ecological signal in carbon isotopes reflecting diet preferences and in oxygen isotopes reflecting drinking water sources [33].

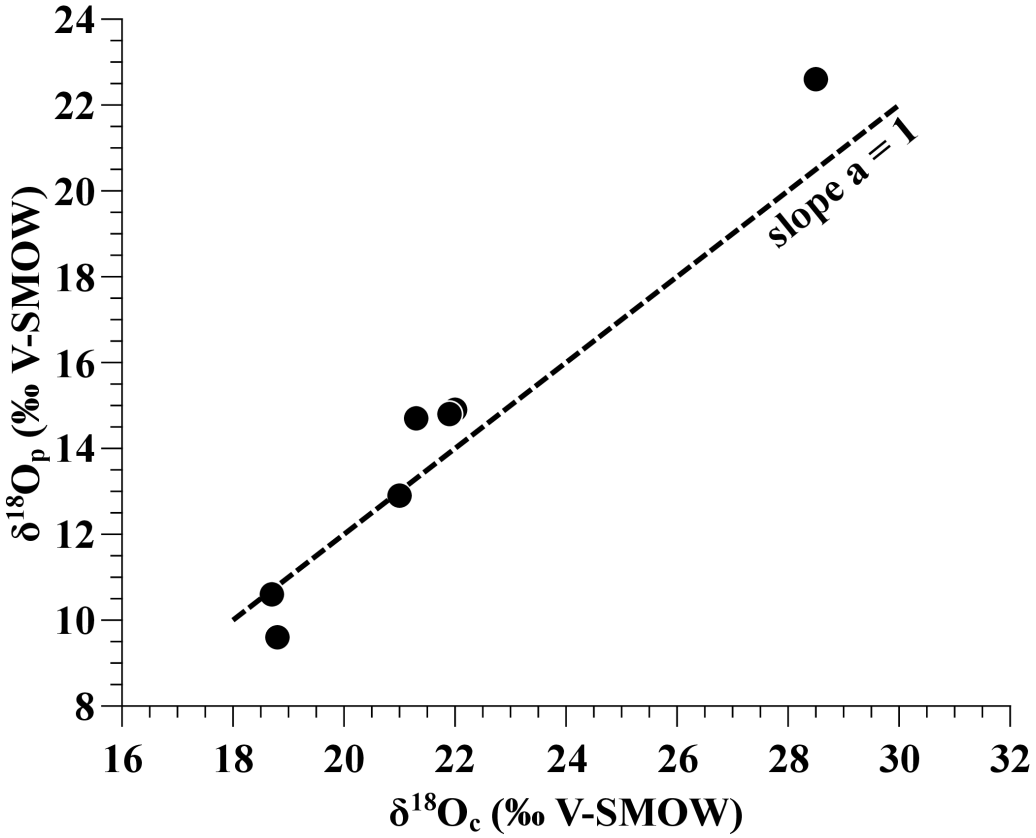

Figure 2. Oxygen isotope compositions of structural carbonate ($\delta^{18}O_c$) of all analyzed vertebrate apatites plotted against their corresponding oxygen isotope compositions of phosphate ($\delta^{18}O_p$).

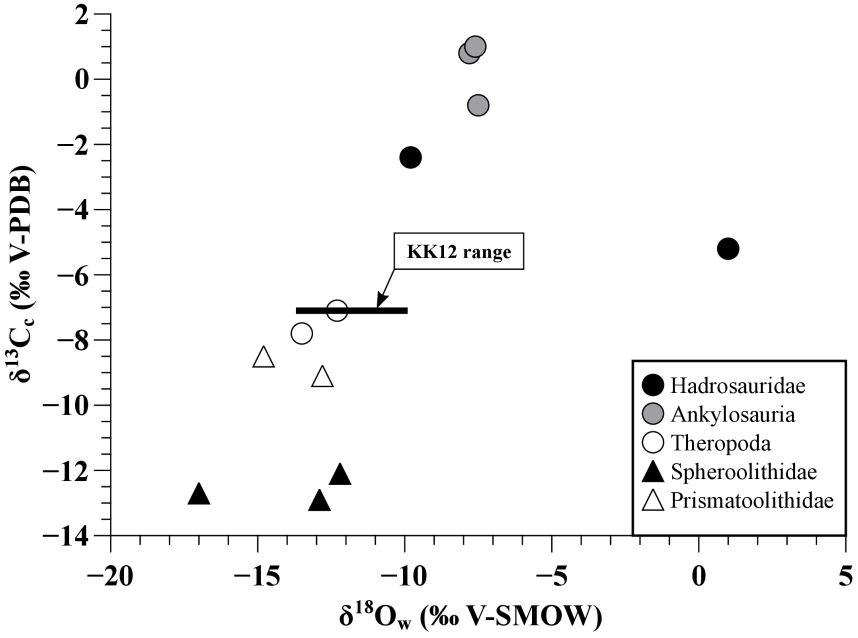

Figure 3. Oxygen isotope compositions of local water ($\delta^{18}O_w$) estimated from the $\delta^{18}O_c$ values of dinosaur eggshells (triangles) and tooth apatite phosphate (circles), reported against the carbon isotope compositions of eggshell calcite or tooth apatite carbonate ($\delta^{13}C_c$). The black horizontal bar corresponds to the range of water $\delta^{18}O_w$ values estimated from the intra-tooth $\delta^{18}O_p$ value variation measured on the tyrannosaurid tooth KK12 [27].

Therefore, we consider that both oxygen and carbon isotope compositions of fossil teeth and eggshells are mostly pristine and can be interpreted in terms of dinosaur ecology and environmental conditions.

4.2. Environmental Conditions in the Kakanaut Area during the Latest Cretaceous

In a recent quantitative analysis of the Kakanaut palaeoflora using the Climate Leaf Analysis Multivariate Program (CLAMP), Zolina et al. [10] calculated a mean annual air temperature (MAAT) of 12.2 ± 2.0 °C for the Kakanaut area, located during the Maastrichtian at a paleolatitude of about 75° N [40]. This temperature of 12.2 ± 2.0 °C would correspond today to a mean annual meteoric water $\delta^{18}O_{mw}$ value of −8.4 ± 1.0‰, according to the recently established $\delta^{18}O_{mw}$–MAAT relationship [55]. Interestingly, the average local environmental water $\delta^{18}O_w$ value estimated from the $\delta^{18}O_p$ values of dinosaur phosphates has a similar value of −8.2 ± 4.7‰ (N = 7). Dinosaur teeth are continuously replaced during life and take several months to grow [56], thus recording in their bulk oxygen isotope composition of phosphate an average of the water $\delta^{18}O_w$ values ingested slightly before and during their mineralization time. Such a pattern was evidenced by the seasonal $\delta^{18}O_p$ variations previously measured along the growth axis of various dinosaur teeth [27,57,58]. It can, therefore, be assumed that the average $\delta^{18}O_p$ value of dinosaur teeth reflects the mean $\delta^{18}O_w$ value of local surface waters and that these ingested waters are of meteoric origin. The consistency of both air temperatures provided by Zolina et al. [10] and $\delta^{18}O_w$ value estimated from dinosaur $\delta^{18}O_p$ can be tested using the $\delta^{18}O_p$ value measured on three bulk scales of lepisosteids (Table 1). The measured value of 14.2‰ indicates that these scales have mineralized from the local water $\delta^{18}O_w$ value of −8.2‰ at a temperature of about 17 °C according to the phosphate–water temperature scale proposed by Lécuyer et al. [59]. This temperature is higher than the mean annual temperature of 12.2 °C but close to the warmest month mean temperature of 20.6 ± 2.5 °C estimated using the CLAMP method [10]. Considering that the optimal growth period of extant lepisosteids occurs during the warm season [60], the measured $\delta^{18}O_p$ value is consistent with the rest of the dataset and the temperature estimates provided by Zolina et al. [10]. We can reasonably consider that the sinusoid-like seasonal pattern in mean annual temperatures and meteoric water $\delta^{18}O_{mw}$ values experienced today at mid to high latitudes [61] prevailed during the Cretaceous [27,58,62]. It follows that the calculated average meteoric water $\delta^{18}O_{mw}$ annual value of about −8.2‰ would also correspond to the values recorded during the inter-seasons (mid-spring or mid-autumn). The anomalously high $\delta^{18}O_p$ value of the tooth KK06 will need further studies beyond the scope of this paper to be correctly interpreted. All we can speculate is that this value may hint at a migratory behavior of this individual that likely spent some time in more arid areas, such as more inland, at lower latitude or in highland regions, while ingesting vegetation characterized by ^{18}O-enriched leaf water due to local evaporation and low amount of precipitation. In such areas, leaf water can be ^{18}O-enriched by up to 20‰ relative to local rainwater or groundwater [63].

Considering the reconstructed range in $\delta^{18}O_{mw}$ values for the Kakanaut area during the latest Cretaceous, the very low water $\delta^{18}O_w$ values ranging from −17.0 to −12.2‰, derived from the $\delta^{18}O_c$ values of eggshell carbonates of the two ootaxa Spheroolithidae and Prismatoolithidae, most likely represent winter waters. The Kakanaut dinosaurs probably laid their eggs at the beginning of spring because egg laying during winter seems unlikely due to freezing temperatures, prolonged or near darkness lasting about 2–3 months [8,9] and limited food availability. The waters ingested by egg-laying females and characterized by a winter isotopic signature could correspond to melted snow supplying local rivers and lakes.

The carbon isotope compositions of teeth and eggshells may also support an egg-laying period at the beginning of spring. Considering that spheroolithid eggs were laid by hadrosaurs and prismatoolithid ones by theropods [11], measured eggshell $\delta^{13}C_c$ values are lower than those of the teeth of corresponding taxa (Figure 3), implying a consumption of food with a lower $\delta^{13}C$ value prior to or during eggshell mineralization. It has been

documented that leaf $\delta^{13}C$ values of C_3 plants vary seasonally, with late spring and summer leaves having $\delta^{13}C$ values up to 6‰ higher than autumn leaves [64], but this tendency does not seem to be a general trend [65]. This high seasonal variability in extant C_3 leaf $\delta^{13}C$ values could at least partly explain the 6.2‰ range of measured carbon isotope compositions of herbivorous dinosaur teeth (hadrosaurs and ankylosaurs), reflecting different timing and periods of tooth mineralization. It has also been observed that spring buds also have a $\delta^{13}C$ value that can be significantly lower than leaves growing later during the year [66]. Seasonal variations in $\delta^{13}C$ values of leaves available for consumption, therefore, suggest that females consumed available early spring foliage when they produced their eggs.

Studies on the duration of egg incubation among dinosaurs show contrasting results. The duration has been estimated to last from a few weeks for small dinosaurs to three months for larger ones based on the size of the hatchling and assuming that dinosaurs possessed a bird-grade physiology [19]. Incubation lasting up to 6 months has also been estimated for some hadrosaurids based on daily incremental line count in tooth dentine that would imply a slow, reptile-grade development [18]. Whatever incubation duration is considered, laying eggs at the very beginning of spring would allow high latitude dinosaurs enough time for the hatchlings to benefit from a maximized period during which food availability and climate were most favorable for survival (Figure 4). It would allow them to reach a body size large enough to tolerate the harsh next winter period, either by migrating to lower latitudes for large species that were biomechanically and energetically capable of doing so or by overwintering under near-freezing to freezing conditions, with limited food availability and prolonged darkness [14,67].

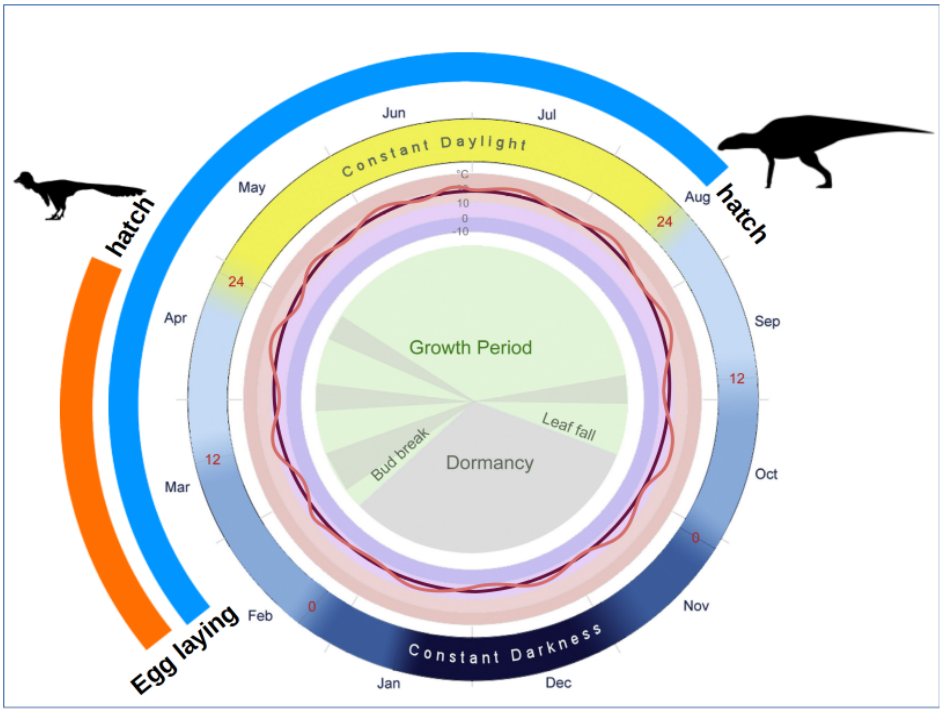

Figure 4. Incubation periods of the eggs from the troodontid (orange arc) and hadrosaurid (blue arc) taxa are drawn based on the present study and the incubation duration estimated for both taxa [18,68], superimposed on the summary graphic of the annual cycle of light, temperature and phenology in the early Maastrichtian at 76° N published by Herman et al. [69]. The outer ring shows the variations in insolation and the red numbers indicate the hours each day (24 h period) when the sun is above the horizon. The inner rings show the temperature regime. The solid red line shows the average temperature variations based on interpolations from the mean annual temperature, the cold month mean and the warm month mean temperatures. The pink line shows the estimated short-term temperature variations based on tree ring data. The center of the diagram shows the proportion of the year when plant growth and dormancy occurred.

Another implication of laying eggs early during spring at high latitudes is that eggs cannot incubate by solar radiance alone, and additional sources of heat have to be used to supplement the need for the embryos to develop under a sufficient incubation temperature. Small theropods and small ornithischians might have been able to brood their eggs by lying on them and transferring their body heat to the clutch [16]. Large species such as tyrannosaurids and hadrosaurids might have used alternative heat sources, such as nest mounds using fermentation of plant debris covering the clutches to warm up the nest [2,8].

This study highlights some crucial aspects of dinosaur reproduction at high latitudes, such as those from the latest Cretaceous Kakanaut area that had to accommodate their reproductive strategies to the challenging environments of high latitudes in terms of timing of egg laying and incubation method.

5. Conclusions

The discovery of Cretaceous dinosaur eggshell fragments in high palaeolatitude localities constitutes the most compelling evidence for their reproductive behavior. Oxygen and carbon stable isotope compositions of eggshell calcite and associated adult teeth apatite provided temporal constraint on the egg-laying strategies used by Kakanaut dinosaurs. Our results show that eggs were most likely laid in early spring, giving time for the hatchling to grow large enough to survive the harsh next winter period and possible southwards migration. Early spring egg laying implies nesting and incubation methods using enhanced heat sources, such as body heat transfer by brooding or nest mounds constructed of plant debris that produced heat by bacterial fermentation. The occurrences of high latitude reproduction among dinosaurs, as well as the inferred egg laying and nesting strategies in these challenging environments, open questions about the global pattern of dinosaur diversity at high latitudes and especially the conspicuous absence of some taxa, such as sauropods, above 50° of latitude [70]. Further studies on nesting strategies used by these dinosaurs might clarify if a causal link exists between their geographic distribution and possible thermal limitations in their egg incubation method and duration.

Author Contributions: Conceptualization, R.A.; Formal analysis, R.A., P.G., J.G. and C.L.; Funding acquisition, R.A.; Investigation, R.A. and L.B.G.; Methodology, F.F.; Resources, L.B.G., P.G., G.G. and A.B.H.; Writing—original draft, R.A.; Writing—review and editing, R.A., L.B.G., P.G., J.G., G.G., C.L., F.F., A.B.H. and R.A.S. All authors have read and agreed to the published version of the manuscript.

Funding: This research was funded by the CNRS INSU program Interrvie (R.A. and C.L.), and by the Brain.be project BR/175/A2/Chicxulub (P.G.).

Institutional Review Board Statement: Not applicable.

Data Availability Statement: Not applicable.

Acknowledgments: This work benefited from fruitful discussions during previous meetings of the UNESCO programs IGCP 608 and 679. Stable isotope compositions of carbonate carbon and oxygen were carried out at the Plateforme d'Ecologie Isotopique du Laboratoire d'Ecologie des Hydrosystèmes Naturels et Anthropisés (LEHNA–UMR5023) member of the RéGEF network.

Conflicts of Interest: The authors declare that they have no conflict of interest.

References

1. Baker, J.R. The Relation between Latitude and Breeding Seasons in Birds. *Proc. Zool. Soc. Lond.* **1939**, *108*, 557–582. [CrossRef]
2. Tanaka, K.; Zelenitsky, D.K.; Therrien, F.; Kobayashi, Y. Nest Substrate Reflects Incubation Style in Extant Archosaurs with Implications for Dinosaur Nesting Habits. *Sci. Rep.* **2018**, *8*, 3170. [CrossRef]
3. Pincheira-Donoso, D.; Bauer, A.M.; Meiri, S.; Uetz, P. Global Taxonomic Diversity of Living Reptiles. *PLoS ONE* **2013**, *8*, e59741. [CrossRef] [PubMed]
4. Artuso, C.; Houston, C.S.; Smith, D.G.; Rohner, C. Great Horned Owl (*Bubo virginianus*), version 1.1. In *Birds of the World*; Sly, N.D., Ed.; Cornell Lab of Ornithology: Ithaca, NY, USA, 2022. [CrossRef]
5. Benkman, C.W. White-winged Crossbill (*Loxia leucoptera*), version 1.0. In *Birds of the World*; Sly, N.D., Ed.; Cornell Lab of Ornithology: Ithaca, NY, USA, 2020. [CrossRef]

6. Buehler, D.A. Bald Eagle (*Haliaeetus leucocephalus*), version 2.0. In *Birds of the World*; Sly, N.D., Ed.; Cornell Lab of Ornithology: Ithaca, NY, USA, 2022. [CrossRef]
7. Carpenter, K. *Eggs, Nests, and Baby Dinosaurs: A Look at Dinosaur Reproduction*; Indiana University Press: Bloomington, IN, USA; Indianapolis, IN, USA, 1999.
8. Spicer, R.A.; Herman, A.B.; Amiot, R.; Spicer, T.E.V. Environmental Adaptations and Constraints on Latest Cretaceous Arctic Dinosaurs. *Glob. Geol.* **2016**, *19*, 241–254. [CrossRef]
9. Spicer, R.A.; Herman, A.B. The Late Cretaceous Environment of the Arctic: A Quantitative Reassessment Based on Plant Fossils. *Palaeogeogr. Palaeoclim. Palaeoecol.* **2010**, *295*, 423–442. [CrossRef]
10. Zolina, A.A.; Golovneva, L.B.; Spicer, R.A. Latest Cretaceous (Maastrichtian) Climate of the Koryak Upland of North-East Russia Based on a Quantitative Analysis of a Palaeo-Polar Flora. *Palaeogeogr. Palaeoclim. Palaeoecol.* **2020**, *560*, 109997. [CrossRef]
11. Godefroit, P.; Golovneva, L.; Shchepetov, S.; Garcia, G.; Alekseev, P. The Last Polar Dinosaurs: High Diversity of Latest Cretaceous Arctic Dinosaurs in Russia. *Naturwissenschaften* **2009**, *96*, 495–501. [CrossRef]
12. Fiorillo, A.R. *Alaska Dinosaurs: An Ancient Arctic World*, 1st ed.; CRC Press: Boca Raton, FL, USA, 2017; ISBN 978-1-138-06087-6.
13. Rich, T.H.; Vickers-Rich, P. *Dinosaurs of Darkness: In Search of the Lost Polar World*, 2nd ed.; Indiana University Press: Bloomington, IN, USA, 2020; ISBN 978-0-253-04739-7.
14. Druckenmiller, P.S.; Erickson, G.M.; Brinkman, D.; Brown, C.M.; Eberle, J.J. Nesting at Extreme Polar Latitudes by Non-Avian Dinosaurs. *Curr. Biol.* **2021**, *31*, 3469–3478.e5. [CrossRef]
15. Chiarenza, A.A.; Fiorillo, A.R.; Tykoski, R.S.; McCarthy, P.J.; Flaig, P.P.; Contreras, D.L. The First Juvenile Dromaeosaurid (Dinosauria: Theropoda) from Arctic Alaska. *PLoS ONE* **2020**, *15*, e0235078. [CrossRef]
16. Amiot, R.; Wang, X.; Wang, S.; Lécuyer, C.; Mazin, J.-M.; MO, J.; Flandrois, J.-P.; Fourel, F.; Wang, X.; Xu, X.; et al. δ^{18}O-Derived Incubation Temperatures of Oviraptorosaur Eggs. *Palaeontology* **2017**, *60*, 633–647. [CrossRef]
17. Bi, S.; Amiot, R.; Peyre de Fabrègues, C.; Pittman, M.; Lamanna, M.C.; Yu, Y.; Yu, C.; Yang, T.; Zhang, S.; Zhao, Q.; et al. An Oviraptorid Preserved atop an Embryo-Bearing Egg Clutch Sheds Light on the Reproductive Biology of Non-Avialan Theropod Dinosaurs. *Sci. Bull.* **2021**, *66*, 947–954. [CrossRef] [PubMed]
18. Erickson, G.M.; Zelenitsky, D.K.; Kay, D.I.; Norell, M.A. Dinosaur Incubation Periods Directly Determined from Growth-Line Counts in Embryonic Teeth Show Reptilian-Grade Development. *Proc. Natl. Acad. Sci. USA* **2017**, *114*, 540–545. [CrossRef] [PubMed]
19. Lee, S.A. Incubation Times of Dinosaur Eggs via Embryonic Metabolism. *Phys. Rev. E* **2016**, *94*, 022402. [CrossRef] [PubMed]
20. Longinelli, A. Oxygen Isotopes in Mammal Bone Phosphate: A New Tool for Paleohydrological and Paleoclimatological Research? *Geochim. Cosmochim. Acta* **1984**, *48*, 385–390. [CrossRef]
21. Longinelli, A.; Nuti, S. Revised Phosphate-Water Isotopic Temperature Scale. *Earth Planet. Sci. Lett.* **1973**, *19*, 373–376. [CrossRef]
22. Kohn, M.J. Predicting Animal δ^{18}O: Accounting for Diet and Physiological Adaptation. *Geochim. Cosmochim. Acta* **1996**, *60*, 4811–4829. [CrossRef]
23. Langlois, C.; Simon, L.; Lécuyer, C. Box-Modeling of Bone and Tooth Phosphate Oxygen Isotope Compositions as a Function of Environmental and Physiological Parameters. *Isot. Environ. Health Stud.* **2003**, *39*, 259–272. [CrossRef]
24. Amiot, R.; Angst, D.; Legendre, S.; Buffetaut, E.; Fourel, F.; Adolfssen, J.; André, A.; Bojar, A.V.; Canoville, A.; Barral, A.; et al. Oxygen Isotope Fractionation between Bird Bone Phosphate and Drinking Water. *Sci. Nat.* **2017**, *104*, 47. [CrossRef]
25. Lazzerini, N.; Lécuyer, C.; Amiot, R.; Angst, D.; Buffetaut, E.; Fourel, F.; Daux, V.; Betancort, J.F.; Sánchez-Marco, A.; Lomoschitz, A. Oxygen Isotope Fractionation between Bird Eggshell Calcite and Body Water: Application to Fossil Eggs from Lanzarote (Canary Islands). *Sci. Nat.* **2016**, *103*, 81. [CrossRef]
26. Dansgaard, W. Stable Isotopes in Precipitation. *Tellus* **1964**, *16*, 436–468. [CrossRef]
27. Goedert, J.; Amiot, R.; Boudad, L.; Buffetaut, E.; Fourel, F.; Godefroit, P.; Kusuhashi, N.; Suteethom, V.; Tong, H.; Watanabe, M.E.; et al. Preliminary Investigation of Seasonal Patterns Recorded in the Oxygen Isotope Composition of Theropod Dinosaur Tooth Enamel. *Palaios* **2016**, *31*, 10–19. [CrossRef]
28. Passey, B.H.; Robinson, T.F.; Ayliffe, L.K.; Cerling, T.E.; Sponheimer, M.; Dearing, M.D.; Roeder, B.L.; Ehleringer, J.R. Carbon Isotope Fractionation between Diet, Breath CO_2, and Bioapatite in Different Mammals. *J. Archaeol. Sci.* **2005**, *32*, 1459–1470. [CrossRef]
29. Ehleringer, J.R.; Monson, R.K. Evolutionary and Ecological Aspects of Photosynthetic Pathway Variation. *Annu. Rev. Ecol. Syst.* **1993**, *24*, 411–439. [CrossRef]
30. Tipple, B.J.; Pagani, M. The Early Origins of Terrestrial C4 Photosynthesis. *Annu. Rev. Earth Planet. Sci.* **2007**, *35*, 435–461. [CrossRef]
31. Farquhar, G.D.; Ehleringer, J.R.; Hubick, K.T. Carbon Isotope Discrimination and Photosynthesis. *Annu. Rev. Plant Physiol. Plant Mol. Biol.* **1989**, *40*, 503–537. [CrossRef]
32. Angst, D.; Lécuyer, C.; Amiot, R.; Buffetaut, E.; Fourel, F.; Martineau, F.; Legendre, S.; Abourachid, A.; Herrel, A. Isotopic and Anatomical Evidence of an Herbivorous Diet in the Early Tertiary Giant Bird *Gastornis*. Implications for the Structure of Paleocene Terrestrial Ecosystems. *Naturwissenschaften* **2014**, *101*, 313–322. [CrossRef]
33. Fricke, H.C.; Rogers, R.R.; Backlund, R.; Dwyer, C.N.; Echt, S. Preservation of Primary Stable Isotope Signals in Dinosaur Remains, and Environmental Gradients of the Late Cretaceous of Montana and Alberta. *Palaeogeogr. Palaeoclim. Palaeoecol.* **2008**, *266*, 13–27. [CrossRef]

34. Fricke, H.C.; Pearson, D.A. Stable Isotope Evidence for Changes in Dietary Niche Partitioning among Hadrosaurian and Ceratopsian Dinosaurs of the Hell Creek Formation, North Dakota. *Paleobiology* **2008**, *34*, 534–552. [CrossRef]
35. Domingo, L.; Barroso-Barcenilla, F.; Cambra-Moo, O. Seasonality and Paleoecology of the Late Cretaceous Multi-Taxa Vertebrate Assemblage of "Lo Hueco" (Central Eastern Spain). *PLoS ONE* **2015**, *10*, e0119968. [CrossRef] [PubMed]
36. Tütken, T. The Diet of Sauropod Dinosaurs: Implications from Carbon Isotope Analysis of Teeth, Bones, and Plants. In *Biology of the Sauropod Dinosaurs: Understanding the Life of Giants*; Klein, N., Remes, K., Sander, M., Eds.; Indiana University Press: Bloomington, IN, USA, 2011; pp. 57–79.
37. Golovneva, L.B.; Gnilovskaya, A.A. Fossil Plants from the Vysokorechenskaya Formation (the Upper Cretaceous, Koryak Upland). *Palaeobotany* **2015**, *6*, 36–47. [CrossRef]
38. Golovneva, L.B.; Shczepetov, S.V. Stratigraphy of the Maastrichtian Deposits of the Kakanaut River Basin (Eastern Part or the Koryak Upland). *Palaeobotany* **2010**, *1*, 96–119. [CrossRef]
39. Shczepetov, S.V.; Herman, A.B. The Formation Conditions of the Burial Site of Late Cretaceous Dinosaurs and Plants in the Kakanaut River Basin (Koryak Highlands, Northeastern Asia). *Strat. Geol. Correl.* **2017**, *25*, 400–418. [CrossRef]
40. Torsvik, T.H.; Van der Voo, R.; Preeden, U.; Mac Niocaill, C.; Steinberger, B.; Doubrovine, P.V.; van Hinsbergen, D.J.J.; Domeier, M.; Gaina, C.; Tohver, E.; et al. Phanerozoic Polar Wander, Palaeogeography and Dynamics. *Earth Sci. Rev.* **2012**, *114*, 325–368. [CrossRef]
41. Scotese, C.R. PALEOMAP PaleoAtlas for Gplates and the PaleoData Plotter Program, PALEOMAP Project. 2016. Available online: https://www.earthbyte.org/paleomap-paleoatlas-for-gplates/ (accessed on 22 April 2022).
42. Lécuyer, C. Oxygen Isotope Analysis of Phosphate. In *Handbook of Stable Isotope Analytical Techniques*; Elsevier: Amsterdam, The Netherlands, 2004; pp. 482–496.
43. Lécuyer, C.; Grandjean, P.; O'Neil, J.R.; Cappetta, H.; Martineau, F. Thermal Excursions in the Ocean at the Cretaceous-Tertiary Boundary (Northern Morocco): $\delta^{18}O$ Record of Phosphatic Fish Debris. *Palaeogeogr. Palaeoclim. Palaeoecol.* **1993**, *105*, 235–243. [CrossRef]
44. Hut, G. Consultants' Group Meeting on Stable Isotope Reference Samples for Geochemical and Hydrological Investigations. 1987. Available online: http://www.Iaea.org/inis/collection/NCLCollectionStore/_Public/18/075/18075746.Pdf (accessed on 22 April 2022).
45. Koch, P.L.; Tuross, N.; Fogel, M.L. The Effects of Sample Treatment and Diagenesis on the Isotopic Integrity of Carbonate in Biogenic Hydroxylapatite. *J. Archaeol. Sci.* **1997**, *24*, 417–429. [CrossRef]
46. Fourel, F.; Martineau, F.; Tóth, E.E.; Görög, A.; Escarguel, G.; Lécuyer, C. Carbon and Oxygen Isotope Variability among Foraminifera and Ostracod Carbonated Shells. *Ann. Univ. Mariae Curie Sklodowska Sect. AAA Phys.* **2016**, *70*, 133–156.
47. Lécuyer, C.; Bogey, C.; Garcia, J.-P.; Grandjean, P.; Barrat, J.A.; Floquet, M.; Bardet, N.; Pereda-Superbiola, X. Stable Isotope Composition and Rare Earth Element Content of Vertebrate Remains from the Late Cretaceous of Northern Spain (Laño): Did the Environmental Record Survive? *Palaeogeogr. Palaeoclim. Palaeoecol.* **2003**, *193*, 457–471. [CrossRef]
48. Bryant, D.J.; Koch, P.L.; Froelich, P.N.; Showers, W.J.; Genna, B.J. Oxygen Isotope Partitioning between Phosphate and Carbonate in Mammalian Apatite. *Geochim. Cosmochim. Acta* **1996**, *60*, 5145–5148. [CrossRef]
49. Iacumin, P.; Bocherens, H.; Mariotti, A.; Longinelli, A. Oxygen Isotope Analyses of Co-Existing Carbonate and Phosphate in Biogenic Apatite: A Way to Monitor Diagenetic Alteration of Bone Phosphate? *Earth Planet. Sci. Lett.* **1996**, *142*, 1–6. [CrossRef]
50. Lécuyer, C.; Balter, V.; Martineau, F.; Fourel, F.; Bernard, A.; Amiot, R.; Gardien, V.; Otero, O.; Legendre, S.; Panczer, G. Oxygen Isotope Fractionation between Apatite-Bound Carbonate and Water Determined from Controlled Experiments with Synthetic Apatites Precipitated at 10–37 °C. *Geochim. Cosmochim. Acta* **2010**, *74*, 2072–2081. [CrossRef]
51. Brudevold, F.; Soremark, R. Chemistry of the Mineral Phase of Enamel. In *Structural and Chemical Organization of Teeth, Volume 2*; Mills, A., Ed.; Elsevier: Amsterdam, The Netherlands, 1967; pp. 247–277.
52. Rink, W.J.; Schwarcz, H.P. Tests for Diagenesis in Tooth Enamel: ESR Dating Signals and Carbonate Contents. *J. Archaeol. Sci.* **1995**, *22*, 251–255. [CrossRef]
53. Vennemann, T.W.; Hegner, E.; Cliff, G.; Benz, G.W. Isotopic Composition of Recent Shark Teeth as a Proxy for Environmental Conditions. *Geochim. Cosmochim. Acta* **2001**, *65*, 1583–1599. [CrossRef]
54. Graf, J.; Tabor, N.J.; Ferguson, K.; Winkler, D.A.; Lee, Y.-N.; May, S.; Jacobs, L.L. Diagenesis of Dinosaur Eggshell from the Gobi Desert, Mongolia. *Palaeogeogr. Palaeoclimatol. Palaeoecol.* **2018**, *494*, 65–74. [CrossRef]
55. Lécuyer, C. *Water on Earth: Physicochemical and Biological Properties*; Wiley-ISTE: London, UK, 2014; ISBN 978-1-84821-477-4.
56. Erickson, G.M. Incremental Lines of von Ebner in Dinosaurs and the Assessment of Tooth Replacement Rates Using Growth Line Counts. *Proc. Natl. Acad. Sci. USA* **1996**, *93*, 14623–14627. [CrossRef] [PubMed]
57. Stanton-Thomas, K.J.; Carlson, S.J. Microscale $\delta^{18}O$ and $\delta^{13}C$ Isotopic Analysis of an Ontogenetic Series of the Hadrosaurid Dinosaur *Edmontosaurus*: Implications for Physiology and Ecology. *Palaeogeogr. Palaeoclim. Palaeoecol.* **2004**, *206*, 257–287. [CrossRef]
58. Straight, W.H.; Barrick, R.E.; Eberth, D.A. Reflections of Surface Water, Seasonality and Climate in Stable Oxygen Isotopes from Tyrannosaurid Tooth Enamel. *Palaeogeogr. Palaeoclim. Palaeoecol.* **2004**, *206*, 239–256. [CrossRef]
59. Lécuyer, C.; Amiot, R.; Touzeau, A.; Trotter, J. Calibration of the Phosphate $\delta^{18}O$ Thermometer with Carbonate–Water Oxygen Isotope Fractionation Equations. *Chem. Geol.* **2013**, *347*, 217–226. [CrossRef]

60. Love, J.W. Age, Growth, and Reproduction of Spotted Gar, *Lepisosteus Oculatus* (Lepisosteidae), from the Lake Pontchartrain Estuary, Louisiana. *Southwest. Nat.* **2004**, *49*, 18–23. [CrossRef]
61. IAEA/WMO Global Network of Isotopes in Precipitation. The GNIP Database. 2022. Available online: https://nucleus.iaea.org/wiser (accessed on 22 April 2022).
62. Spicer, R.; Valdes, P.; Hughes, A.; Yang, J.; Spicer, T.; Herman, A.; Farnsworth, A. New Insights into the Thermal Regime and Hydrodynamics of the Early Late Cretaceous Arctic. *Geol. Mag.* **2020**, *157*, 1729–1746. [CrossRef]
63. Zhan, L.; Chen, J.; Li, L.; Xin, P. Plant Water Use Strategies Indicated by Isotopic Signatures of Leaf Water: Observations in Southern and Northern China. *Agric. For. Meteorol.* **2019**, *276–277*, 107624. [CrossRef]
64. Lowdon, J.A.; Dyck, W. Seasonal Variations in the Isotope Ratios of Carbon in Maple Leaves and Other Plants. *Can. J. Earth Sci.* **1974**, *11*, 79–88. [CrossRef]
65. Metcalfe, J.Z. C_3 Plant Isotopic Variability in a Boreal Mixed Woodland: Implications for Bison and Other Herbivores. *PeerJ* **2021**, *9*, e12167. [CrossRef] [PubMed]
66. Suh, Y.J.; Diefendorf, A.F. Seasonal and Canopy Height Variation in N-Alkanes and Their Carbon Isotopes in a Temperate Forest. *Org. Geochem.* **2018**, *116*, 23–34. [CrossRef]
67. Bell, P.R.; Snively, E. Polar Dinosaurs on Parade: A Review of Dinosaur Migration. *Alcheringa Australas. J. Palaeontol.* **2008**, *32*, 271–284. [CrossRef]
68. Varricchio, D.J.; Kundrát, M.; Hogan, J. An Intermediate Incubation Period and Primitive Brooding in a Theropod Dinosaur. *Sci. Rep.* **2018**, *8*, 12454. [CrossRef]
69. Herman, A.B.; Spicer, R.A.; Spicer, T.E.V. Environmental Constraints on Terrestrial Vertebrate Behaviour and Reproduction in the High Arctic of the Late Cretaceous. *Palaeogeogr. Palaeoclim. Palaeoecol.* **2016**, *441*, 317–338. [CrossRef]
70. Chiarenza, A.A.; Mannion, P.D.; Farnsworth, A.; Carrano, M.T.; Varela, S. Climatic Constraints on the Biogeographic History of Mesozoic Dinosaurs. *Curr. Biol.* **2022**, *32*, 570–585.e3. [CrossRef]